Single board computer and adapted 3D-printed case-based low cost and compact optical coherence tomography

Daewoon Seong[a], Sangyeob Han[b], Yoonseok Kim[a], Juyeon Hong[a], Ruchire Eranga Wijhesinghe[c,d], Mansik Jeon[a,*], and Jeehyun Kim[a]

[a] School of Electronic and Electrical Engineering, Kyungpook National University, 80 Daehak-ro, Buk-gu, Daegu 41566, Republic of Korea

[b] ICT Convergence Research Center, Kyungpook National University, 80, Daehak-ro, Buk-gu, Daegu 41566, Republic of Korea

[c] Department of Electrical and Electronic Engineering, Faculty of Engineering, Sri Lanka Institute of Information Technology, Malabe 10115, Sri Lanka

[d] Center for Excellence in Intelligent Informatics, Electronics & Transmission (CIET), Sri Lanka Institute of Information Technology, Malabe 10115, Sri Lanka

ABSTRACT

Optical coherence tomography (OCT) is a non-invasive, label-free imaging method based on high-resolution interferometric optics that allows real-time visualization of morphological structures and depth-resolved images. The high cost of most commercially available OCT systems limits their widespread use, especially in resource-poor settings. Miniaturization of OCT devices therefore reduces not only size but also cost and has the potential to open new markets for this technology. In this study, we developed a small, portable 3D printed OCT system (SBC-OCT) based on a single-board computer. To reduce the cost to configure the system, the whole case of SBC-OCT is made with 3D-printed architecture. Using an area camera to avoid thermally induced alignment distortions in the spectrometer during system operation, the spectrometer is temperature insensitive, requires no hardware changes or additional components, and requires minimal computational effort. An applied automatic signal correction method was developed. The smaller size, lighter weight, and lower cost of SBC-OCT highlight its significant relevance in medical, industrial, and security applications, showcasing its potential for broad adoption.

Keywords: Temperature-insensitive optical coherence tomography; Compact optical coherence tomography; Automatic peak detection, Latte Panda single-board computer

1. INTRODUCTION

Optical coherence tomography (OCT) is an advanced imaging technique that uses non-invasive, label-free, high-resolution interferometry to deliver real-time information about the morphology and structure of samples, as well as depth-resolved imaging [1]. OCT has been widely adopted in diverse fields, including medicine [2-6], industry [7, 8], and agriculture [9, 10]. Nevertheless, the high cost of most commercially available OCT systems has significantly hindered their accessibility, especially in settings with limited resources. The process of miniaturizing OCT systems involves addressing three primary considerations: (1) reducing size, (2) lowering cost, and (3) minimizing weight [11]. Moreover, depending on the intended application, compact OCT systems may require not only size reduction but also enhanced flexibility or further cost efficiency [11].

Since the introduction of Fourier-domain OCT, two primary types, known as spectral-domain OCT (SD-OCT) and swept-source OCT (SS-OCT), have been predominantly utilized. While both systems share a similar theoretical foundation, they differ in their methods for measuring interference signals and in hardware requirements, leading to trade-offs between imaging performance and cost [12]. SS-OCT, despite its superior performance, faces significant cost challenges in miniaturization due to the complexity of its swept laser source (narrow-band laser with a rapidly tunable center frequency) and the need for a high-performance digitizer capable of converting interference signals into digital data at high sampling rates [13, 14]. On the other hand, SD-OCT, which utilizes a broadband light source and

Optics and Biophotonics in Low-Resource Settings XI, edited by David Levitz,
Aydogan Ozcan, Proc. of SPIE Vol. 13307, 1330707 · © 2025 SPIE
1605-7422 · doi: 10.1117/12.3041806

spectrometer-based detection, offers a simpler configuration. This simplicity makes it more cost-effective and better suited for developing low-cost OCT systems [12, 15].

In SD-OCT systems, the spectrometer is a crucial component that directly impacts image quality but is also one of the largest and most complex parts of the overall setup [11, 12]. One early attempt to miniaturize the OCT system involved modifying a commercial spectrometer by integrating a faster line-scan camera, achieving a 10 kHz A-scan rate within a compact design [16]. However, further adjustments were necessary to align the camera with the commercial spectrometer to enhance sensitivity. Additionally, a fully customized, low-cost spectrometer design was developed using 3D printing technology, offering improved tolerance for vertical misalignment [17]. This approach, however, required averaging multiple frames to enhance the signal-to-noise ratio. Arrayed waveguide gratings (AWGs) have also been explored as an alternative for spectrometer design [18]. While AWG-based spectrometers show strong potential for creating ultra-compact, portable, and low-cost OCT systems, they currently face challenges such as a limited number of channels, narrower bandwidths, and higher transmission losses compared to traditional diffraction gratings. Further improvements are needed to address these limitations.

In this study, we developed a compact OCT system (SBC-OCT) based on a single-board computer and a temperature-insensitive spectrometer. To mitigate alignment distortions in the spectrometer caused by heat generated during system operation, we implemented an automatic signal compensation method utilizing an area-scan camera. This approach enabled the integration of a temperature-insensitive spectrometer into the SBC-OCT system.

2. MATERIALS AND METHODS

2.1 System configuration of SBC-OCT

The hardware configuration of the SBC-OCT system, including the interferometer setup and a photograph of the packaged system, is shown in Fig. 1. The optical design of the SBC-OCT system employed a Michelson interferometer-based SD-OCT setup, integrated with an area-scan camera-based temperature-insensitive (TI) spectrometer. A super-luminescent diode (EXS210022-02, Exalos, Switzerland) with a center wavelength of 840 nm and a bandwidth of 50 nm served as the broadband light source. Light from the source was directed to a 50:50 fiber coupler (TW850R5A2, Thorlabs, USA), splitting it evenly between the reference and sample arms. The reference arm included a collimator (F260APC-780, Thorlabs, USA), a lens (AC254-050-B, Thorlabs, USA), and a mirror (PF10-03-P01, Thorlabs, USA). Similarly, the sample arm consisted of equivalent optical components but included an additional galvanometer scanner (GVS002, Thorlabs, USA) for 3D scanning. The backscattered light from both arms was combined in the fiber coupler and transmitted to the customized TI-spectrometer. The optical configuration of the TI-spectrometer is detailed in Fig. 1(b), while its photograph is shown in Fig. 1(c), whose overall configuration is structure shares similar characteristics with spectrometer designs used in previous studies [19, 20]. The spectrometer featured a collimator (TC25APC-780, Thorlabs, USA), a diffraction grating (WP-HD1800/840, Wasatch Photonics, USA), a lens (AC254-050-B, Thorlabs, USA), and an area-scan camera (acA2000-165μmNIR, Basler, Germany). The diffraction grating was positioned at a 49° angle to ensure accurate beam propagation. The dispersed light was focused using a lens and then captured by the area-scan camera. The TI-spectrometer had overall dimensions of 140 × 110 × 75 mm³ (width × depth × height). The interfered signal was processed by a data acquisition (DAQ) board (USB-6341, National Instruments, USA), placed on the second layer of the SBC-OCT system. For processing and system control, a Latte Panda single-board computer (dimensions: 115 × 78 × 14 mm³) was used. It synchronized the OCT hardware, including the galvanometer scanner and area-scan camera, via triggers, performed OCT signal processing, and displayed the processed OCT images. This compact configuration significantly reduced the system's size and weight. All hardware components, including the interferometer, drivers, power supply, TI-spectrometer, and Latte Panda single-board computer, were arranged using 3D modeling software to optimize the spatial configuration and minimize the overall volume of the SBC-OCT system. To further reduce manufacturing costs, the system's structure was fabricated using a polylactic acid (PLA)-based 3D printer. The final dimensions of the assembled SBC-OCT system, excluding the display and scanner, are 230 × 230 × 330 mm³ (width × depth × height), with a total production cost of approximately $10,000. All components of the SBC-OCT system were carefully positioned at precise locations based on the 3D model design.

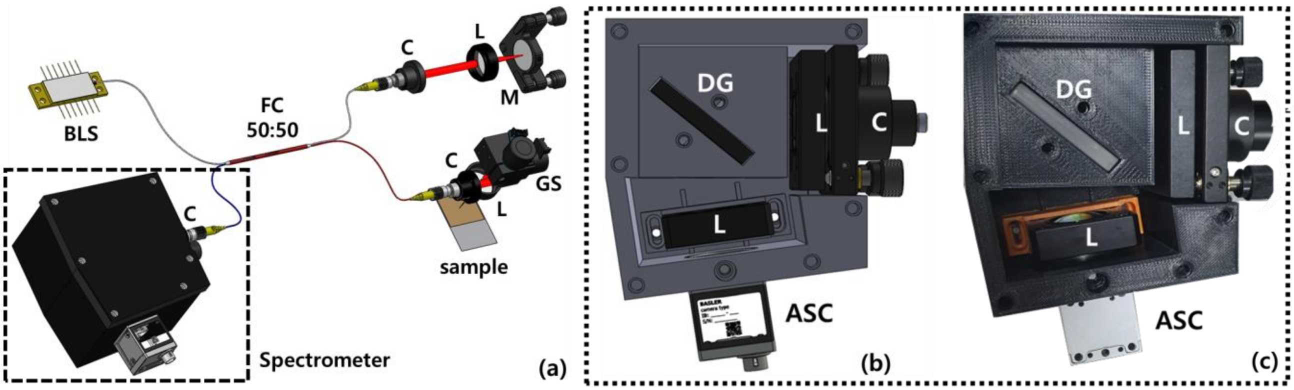

Figure 1. Configuration of the SBC-OCT system utilizing the TI-spectrometer. (a) Detailed hardware components of the OCT system. (b) 3D modeling design of the customized TI-spectrometer, including its optical layout. (c) Photograph of the actual 3D-printed TI-spectrometer. ASC, Area Scan Camera; BLS, Broadband Light Source; C, Collimator; DG, Diffraction Grating; FC, Fiber Coupler; GS, Galvanometer Scanner; L, Lens; M, Mirror.

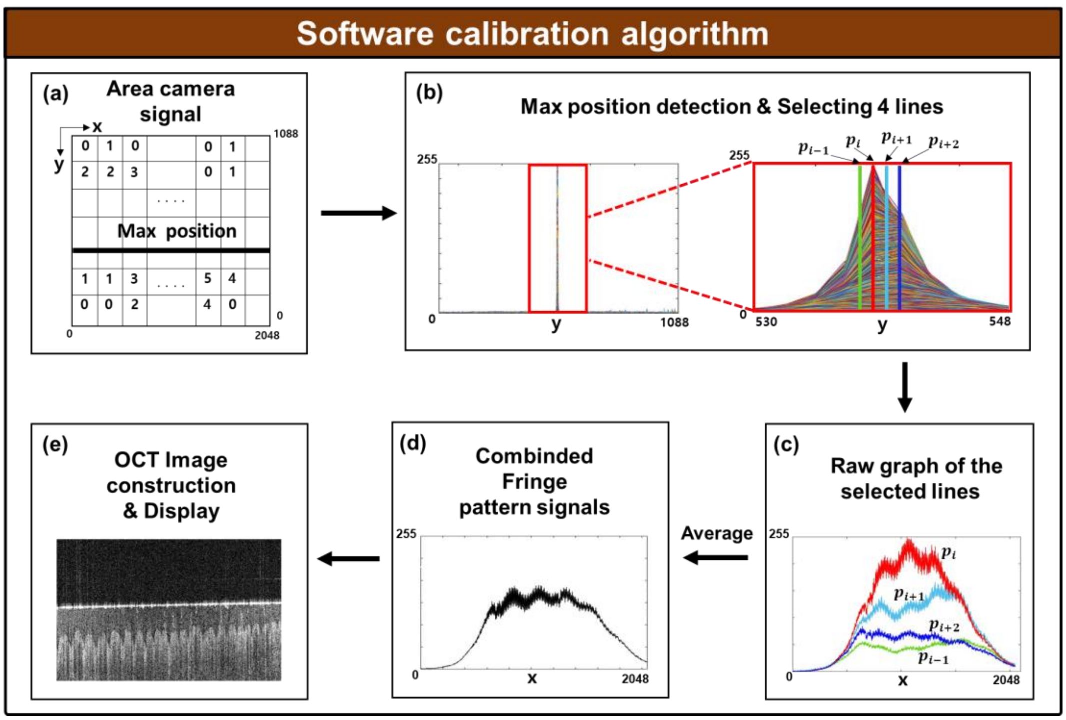

Figure 2. Description of the automatic signal compensation process. (a) Software flowchart of SBC-OCT for TI-spectrometer.

2.2 Signal compensation method of TI-spectrometer

The software flowchart for processing OCT signals through the TI-spectrometer is shown in Fig. 2, with all steps executed on a Latte Panda single-board computer using LabVIEW. The process consists of three stages: (1) data acquisition using the TI-spectrometer with an area-scan camera, (2) OCT signal processing with automatic signal compensation, and (3) real-time image display. Raw signals captured by the area-scan camera (2048 × 1088 pixels) were buffered and transferred for processing, where the peak intensity pixel (P_i) along the x-axis was identified and used for signal extraction. Four pixels (P_{i-1}, P_i, P_{i+1}, and P_{i+2}) were selected and averaged to generate the raw interfered signal, which was subsequently processed through background removal, k-linearization, dispersion compensation, Fourier transform, and log scaling to produce real-time cross-sectional OCT images. The four-pixel selection was optimized to balance image quality and acquisition speed, matching the 10–20 μm cell height of conventional line-scan cameras (using an area-scan camera pixel size of 5.5 μm × 4 = 22 μm) and enhancing acquisition speed by focusing on a specific signal region. The system achieved a frame rate of 10 frames per second with 500 A-scans per B-scan. As shown in Fig. 3, while increasing the number of pixels improved signal intensity, it reduced the camera's maximum acquisition speed, validating the four-pixel choice as an optimal balance between speed and quality for the SBC-OCT system.

3. RESULTS

To quantitatively assess the robustness of the TI-spectrometer-based OCT system against temperature variations and its signal restoration performance, we imaged an IR card as a sample under three conditions: (1) initially aligned (original) image, (2) distorted image (affected by temperature increase), and (3) compensated image (corrected via automatic signal compensation), as shown in Fig. 3. The qualitative analysis of the OCT images (Fig. 3(a)-(c)) clearly highlights the differences between the distorted and compensated states compared to the original image. For quantitative evaluation, A-scan profiling was performed along the depth direction, and image histogram comparisons were made for each region of interest (ROI), marked with red boxes in Fig. 3(a)-(c). Each ROI had dimensions of 200 pixels (X-axis) × 215 pixels (Z-axis). The second column in Fig. 3 (Fig. 3(i)) displays the results of A-scan profiling, where the signal was averaged over 215 lines in the ROI along the X-axis. The A-scan profile for the distorted case (Fig. 3(b-i)) shows an absence of any meaningful OCT signal when compared to the original image (Fig. 3(a-i)), demonstrating the necessity for positional correction. Conversely, the depth signal extracted from the compensated image (Fig. 3(c-i)) reveals restored OCT signals, achieved by shifting the measuring position to the peak pixel. To further analyze signal differences, we subtracted the A-scan profiles of each ROI, with the results presented in the third column of Fig. 3 (Fig. 3(ii)). Since no structured signal was present in the distorted image, subtracting its profile from the original and compensated images (Fig. 3(a-ii) and Fig. 3(b-ii)) produced results nearly identical to the original signal. However, subtracting the original from the compensated signal (Fig. 3(c-ii)) confirms the effectiveness of the automatic signal compensation method, as the subtracted signals remained below the noise level. Additionally, the histograms of the obtained images, shown in the fourth column of Fig. 3 (Fig. 5(iii)), further validate the proposed compensation method's ability to restore distorted signals.

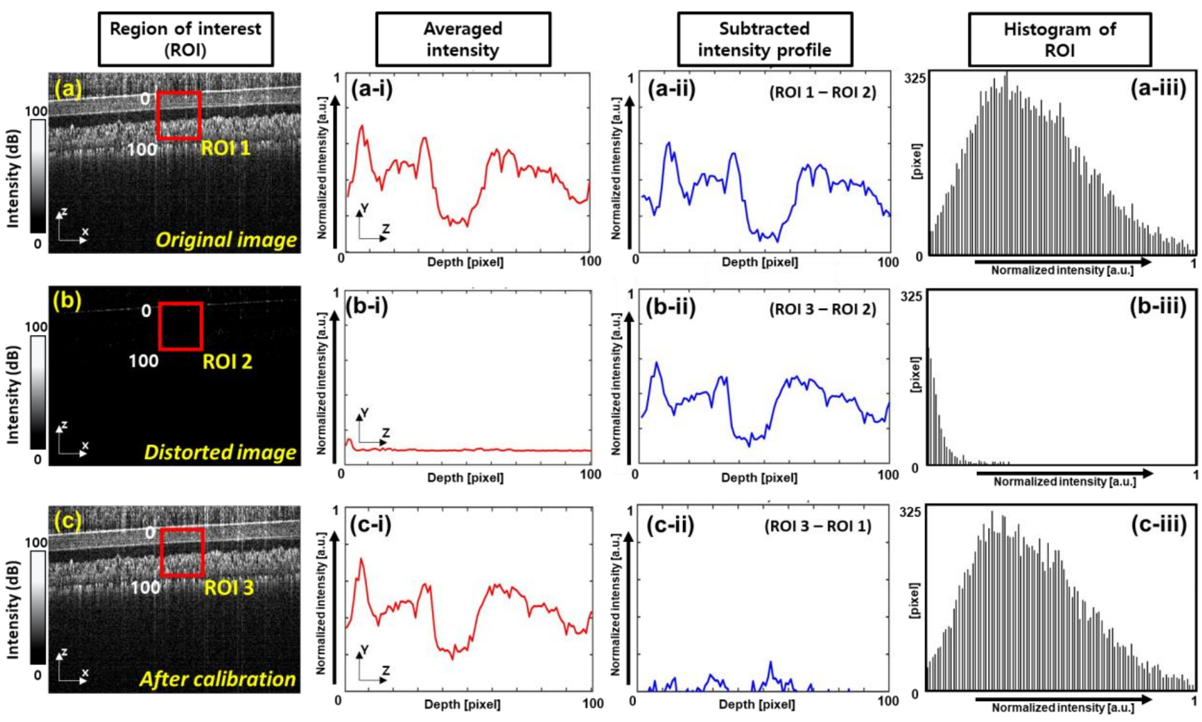

Figure 3. Quantitative performance evaluation of the SBC-OCT system. (a)-(c) 2D-OCT images representing the original, distorted, and compensated states. (i) Depth intensity profiles for ROI 1, ROI 2, and ROI 3. (ii) Average intensity differences between ROI 1 and ROI 2, ROI 3 and ROI 2, and ROI 1 and ROI 3. (iii) Intensity histograms corresponding to (a)-(c). ROI, region of interest.

4. CONCLUSION

In conclusion, we developed a compact OCT system based on the Latte Panda single-board computer, achieving significant reductions in size and weight to improve portability and applicability. All non-optical hardware components were fabricated using a 3D printer, further minimizing cost and complexity. To address alignment distortions caused by thermal effects on the 3D-printed structure, particularly from the heat generated by the camera, an automatic signal compensation method was implemented. This approach required no hardware modifications, no additional components, and imposed minimal computational load. Hence, based on the obtained results demonstrating the applicability and practicality of SBC-OCT, the proposed system presents promising outcomes that could encourage its adoption across various applications, including medical, industrial, and agricultural fields.

ACKNOWLEDGEMENTS

This research was supported by the MSIT(Ministry of Science and ICT), Korea, under the Innovative Human Resource Development for Local Intellectualization support program(IITP-2024-RS-2022-00156389) supervised by the IITP(Institute for Information & communications Technology Planning & Evaluation). In addition, this research was also funded by supported by the BK21 Four project funded by the Ministry of Education, Korea (4199990113966).

REFERENCES

[1] D. Huang, E. A. Swanson, C. P. Lin *et al.*, "Optical coherence tomography," science, 254(5035), 1178-1181 (1991).

[2] W. Drexler, U. Morgner, R. K. Ghanta *et al.*, "Ultrahigh-resolution ophthalmic optical coherence tomography," Nature medicine, 7(4), 502-507 (2001).

[3] D. Seong, E. Lee, Y. Kim *et al.*, "Deep learning based highly accurate transplanted bioengineered corneal equivalent thickness measurement using optical coherence tomography," NPJ Digital Medicine, 7(1), 308 (2024).

[4] C. A. Puliafito, M. R. Hee, C. P. Lin *et al.*, "Imaging of macular diseases with optical coherence tomography," Ophthalmology, 102(2), 217-229 (1995).

[5] D. Seong, S. Han, Y. Kim *et al.*, "Polarization-insensitive optical coherence tomography using polarization maintaining fiber with a simple optical configuration," Photonics Research, 12(10), 2354-2364 (2024).

[6] J. Hong, D. Seong, D. Kang *et al.*, "Imaging of the vascular distribution of the outer ear using optical coherence tomography angiography for highly accurate positioning of a hearable sensor," APL bioengineering, 8(2), (2024).

[7] D. Seong, D. Jeon, R. E. Wijesinghe *et al.*, "Ultrahigh-speed spectral-domain optical coherence tomography up to 1-mhz a-scan rate using space–time-division multiplexing," IEEE Transactions on Instrumentation and Measurement, 70, 1-8 (2021).

[8] R. Su, M. Kirillin, E. W. Chang *et al.*, "Perspectives of mid-infrared optical coherence tomography for inspection and micrometrology of industrial ceramics," Optics express, 22(13), 15804-15819 (2014).

[9] S. A. Saleah, S.-Y. Lee, R. E. Wijesinghe *et al.*, "Optical signal intensity incorporated rice seed cultivar classification using optical coherence tomography," Computers and Electronics in Agriculture, 198, 107014 (2022).

[10] J. Lee, S.-Y. Lee, S. Han *et al.*, "Multi-directional morphological assessment of single bacterial colonies through non-invasive optical imaging," Annals of Biomedical Engineering, 48, 3014-3023 (2020).

[11] E. A. Rank, A. Agneter, T. Schmoll *et al.*, "Miniaturizing optical coherence tomography," Translational Biophotonics, 4(1-2), e202100007 (2022).

[12] G. Song, E. T. Jelly, K. K. Chu *et al.*, "A review of low-cost and portable optical coherence tomography," Progress in Biomedical Engineering, 3(3), 032002 (2021).

[13] I. Grulkowski, J. J. Liu, B. Potsaid *et al.*, "Retinal, anterior segment and full eye imaging using ultrahigh speed swept source OCT with vertical-cavity surface emitting lasers," Biomedical optics express, 3(11), 2733-2751 (2012).

[14] S. Moon, and E. S. Choi, "VCSEL-based swept source for low-cost optical coherence tomography," Biomedical optics express, 8(2), 1110-1121 (2017).

[15] S. A. Saleah, D. Seong, S. Han *et al.*, "Integrated quad-scanner strategy-based optical coherence tomography for the whole-directional volumetric imaging of a sample," Sensors, 21(4), 1305 (2021).

[16] R. Dsouza, J. Won, G. L. Monroy *et al.*, "Economical and compact briefcase spectral-domain optical coherence tomography system for primary care and point-of-care applications," Journal of biomedical optics, 23(9), 096003-096003 (2018).

[17] S. Kim, M. Crose, W. J. Eldridge *et al.*, "Design and implementation of a low-cost, portable OCT system," Biomedical optics express, 9(3), 1232-1243 (2018).

[18] R. M. Ruis, A. Leinse, R. Dekker *et al.*, "Decreasing the size of a spectral domain optical coherence tomography system with cascaded arrayed waveguide gratings in a photonic integrated circuit," IEEE Journal of Selected Topics in Quantum Electronics, 25(1), 1-9 (2018).

[19] D. Seong, S. Han, D. Kang *et al.*, "Development of single board computer-based temperature-insensitive compact optical coherence tomography for versatile applications," IEEE Transactions on Instrumentation and Measurement, (2024).

[20] D. Seong, S. Han, D. Jeon *et al.*, "Dynamic compensation of path length difference in optical coherence tomography by an automatic temperature control system of optical fiber," IEEE Access, 8, 77501-77510 (2020).